ELSEVIER

FEBS Letters 338 (1994) 89–92

FEBS 13570

FEBS LETTERS

Structure and stability of pertussis toxin studied by in situ atomic force microscopy

Jie Yang, Jianxun Mou, Zhifeng Shao*

Bio-SPM Laboratory, Department of Molecular Physiology & Biological Physics and Biophysics Program, University of Virginia, Box 449, Charlottesville, VA 22908, USA

Received 15 November 1993

Abstract

Pertussis toxin, both complete and the B-oligomer, were imaged by atomic force miroscopy (AFM), using specimens prepared by simple surface adsorption on mica without further manipulation. The spatial arrangement of the subunits of the B-oligomer was clearly resolved, representing the first protein quaternary structure obtained by AFM in situ. The results suggest that the B-oligomer is a flat pentamer with the two large subunits located next to each other, and the catalytic A-subunit situated at the center above. We found that the B-pentamer was structurally stable for temperatures up to 60°C and within the pH range of 4.5–9.5. It is also demonstrated that the AFM was capable of resolving features down to 0.5 nm on the B-oligomers, indicating its great potential for structural determination.

Key words: Atomic force microscopy; Pertussis toxin; Structure; Resolution

1. Introduction

Pertussis toxin is produced by *Bordetella pertussis*, which causes whooping cough [1]. Its amino acid sequence has been determined recently [2]. Biochemical studies suggested that the pertussis toxin has the typical A-B structure for bacterial toxins [3–6]. The 26 kDa A-subunit (S1) is believed to be the catalytic subunit. But, different from the well studied cholera toxin [7–10], the 79 kDa pertussis toxin B-oligomer has 5 subunits of different mass, with each of S2 (21.9 kDa), S3 (21.9 kDa), S5 (11 kDa) and two of S4 (12.1 kDa) [2,3]. The A-subunit (S1) is weakly bound to the B-oligomer, which exerts its effect by catalyzing the ADP ribosylation of G-proteins (G_i, G_0 and transducin), upon activation after penetrating the cell membrane [5]. Similar to the cholera toxin, the B-oligomer is believed mainly to facilitate pertussis toxin binding to an unidentified glycoprotein receptor in the cell membrane [11], although it was recently demonstrated that pertussis toxin also bound to the glycolipid GD_{1a} with high affinity [12]. So far, the structure of the pertussis toxin has only been reported from electron microscopy as a ring of 4 or 5 members, insufficient to determine their spatial arrangement [13]. The main difficulty has been the preparation of 2D or 3D crystals for either electron microscopy or X-ray diffraction.

For non-crystallized specimens, the atomic force microscopy (AFM) should be preferred for structural elucidation of macromolecules for its high spatial resolution intrinsic high signal-to-noise ratio, and physiological imaging environments [14–16]. Previously, AFM has already been used to image several membrane proteins at high spatial resolution without extensive specimen manipulation [17–22], e.g. better than 2 nm resolution for non-crystallized cholera toxin on a supported synthetic phospholipid bilayer [20], and 3.5 nm on gap junction fragments [22], among others [17–18]. Recently, we have further demonstrated that for soluble proteins, freshly cleaved mica was an ideal substrate for AFM imaging in solution, which provided sufficient stability to withstand the disturbance of the probe force [23]. In this letter, we report that the same method was successfully applied to the study of pertussis toxin. We found that both intact pertussis toxin and the B-oligomer had a very strong affinity to the negatively charged mica surface, perhaps because their receptors are also negatively charged at normal pH, although it is not clear whether they would bind to negatively charged lipid surfaces as well. Based on the images of AFM in situ, we show that the pertussis toxin B-oligomer is a pentamer with the two large subunits, S2 and S3, located next to each other, while the A subunit is located on top of the B-pentamer at the center. We also show that the B-pentamer remains intact for temperatures up to 60°C, and pH range between 4.5 and 9.5.

*Corresponding author.

SSDI 0014-5793(93)E1487-7

2. Materials and methods

2.1 Materials

Both intact pertussis toxin and the B-oligomer were purchased from Calbiochem (San Diego, CA), List (Campbell, CA), and Sigma (St. Louis, MO). No difference was found in the quality of AFM imaging of toxins from different sources. Ruby mica, as the substrate, was purchased from Ernest F. Fullam Inc. (Latham, NY).

2.2. Specimen Preparation

15 μl protein solution (50 μg/ml, 10 mM sodium phosphate, 50 mM NaCl, pH 7.0 for the B-oligomer; 50 μg/ml, 12.5 mM sodium phosphate, 125 mM NaCl, pH 7.0, 12% glycerol for the complete toxin) was applied to a freshly cleaved mica surface and incubated for about 30 min followed by gentle washing with deionized water. The specimen was never exposed to air and stored at 4°C overnight, and imaged by AFM without further manipulation.

2.3 AFM imaging

All AFM images were obtained with a NanoScope II AFM, using oxide sharpened Si_3N_4 tips with a spring constant of 0.06 N/m (Digital Instruments, Santa Barbara, CA), in solution at room temperature. Most tips showed satisfactory performance. Tracking force was kept typically below 0.3 nN. Scanning speed for most images was 4.73 Hz.

2.4. Image Analysis

Original AFM images of the B-oligomer were first low pass filtered to remove high frequency noises in order to improve alignment accuracy. 300 B-oligomers were selected from 21 AFM images with different specimens and tips. The only criteria for inclusion/exclusion were that the subunits were well resolved and the distortion was not excessive. The program package SPIDER[24] was used to align these images both angularly and laterally. A subset of 8 images was first aligned to obtain the first reference image. The complete set was then aligned against this reference. After the first averaged image was obtained, the complete set was once again aligned with this new averaged image as the reference to obtain the next averaged image. This procedure was repeated, and the difference in the averaged images was not noticeable. In the angular alignment, the masked images were first exponentially expanded to enhance contrast in order to improve computational accuracy, due to the small structural difference in subunits. Prior to summation after image alignment, all images were normalized to have equal weight.

2.5. Stability studies

For the temperature stability studies, both the protein solution and the mica substrate were heated to the selected temperature. After about 10 min, 15 μl of the protein solution was applied to the mica surface, allowed to adsorb for 20 min at the same temperature, followed by slow cooling to room temperature, washed as described before, stored at 4°C overnight, and imaged in deionized water. For the pH stability studies, the pH of the protein solution was adjusted accordingly. After incubation for about 30 min to allow protein adsorption, the solution was washed away and the specimen was stored at 4°C overnight prior to AFM imaging.

3. Results and discussion

Fig. 1a is a typical AFM image of pertussis toxin B-oligomer in deionized water, where the pentameric structure is clearly resolved. This is in sharp contrast to the images of the intact pertussis toxin (Fig. 1b), where the central pore is clearly absent. Both images were the originals without any processing. This indicates that the A-subunit is located at the center of the B-oligomer, similar to the cholera toxin [9,10]. The substructure of the intact pertussis toxin is not well resolved, probably because the A-subunit prevented the tip to sense the subunits of the B-oligomer below, due to its finite size.

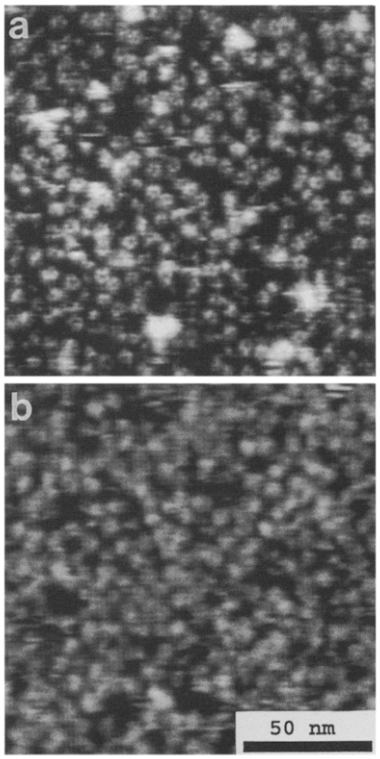

Fig. 1. Original AFM images of pertussis toxin, obtained in deionized water at room temperature. (a) Pertussis toxin B-oligomer. The pentameric structure is well resolved with a central pore on most of these molecules. (b) Pertussis toxin (intact). In contast to the B-oligomer, the central pore is clearly absent from the majority of the molecules, indicating that the catalytic subunit A (S1) is located at the center on top of the B-oligomer. For the intact toxin, stable imaging was more difficult to obtain than the B-oligomer, due to the unstable adhesion force because of the contact of the hydrophobic A-subunit and the tip.

Eight well resolved B-oligomers are shown in Fig. 2a, where two large subunits are almost directly identifiable. 300 such well resolved B-oligomers were selected from 21 AFM micrographs, and the program SPIDER was used to align these images to obtain an averaged image [24,25], as shown in Fig. 2b. The two large subunits are now clearly resolved. If we assume that all subunits are in a compact globular form with similar compressibility, the two large subunits would be identified as the subunits S2 and S3, although alternative interpretation cannot be entirely ruled out. Since the subunits S2 and S4, as well as S3 and S4, remained in the dimer state even after incubation in 5 M urea [3], S5 should then be the one facing the subunits S2 and S3. Based on this result, a model for the pertussis toxin is proposed in Fig. 2c, which favors the view that such an arrangement would allow the amino terminal domain of S2 and S3 to perform other functions, for example, binding with the enzymatically active A-subunit (S1) [2]. The extremely small difference in mass between S2 and S3 prevented the AFM from determining which side of the B-oligomer actually binds the A-subunit. The difference in molecular

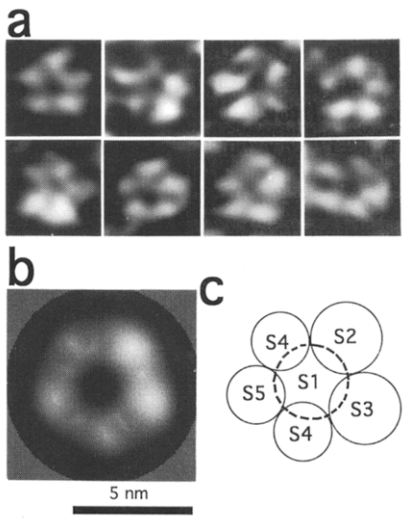

Fig. 2. (a) Eight representative AFM images of the pertussis toxin B-oligomer are shown. Notice that the different size in subunits can be differentiated. (b) The averaged image of 300 pertussis toxin B-oligomers after alignment using SPIDER [24]. It suggests that the two large subunits are located next to each other. The B-pentamer has a diameter of 6.1 nm, comparable to the cholera toxin. The often discussed tip broadening is very small, if not at all, which agrees with a previous finding [23]. (c) The proposed subunit arrangement of the pertussis toxin. Since AFM cannot distinguish between S2 and S3, it is not clear which side the A-subunit is attached.

weight between S4 and S5 is too small to be differentiated by the AFM at present. The average diameter of the pertussis toxin B-oligomer measured from Fig. 2b is ~6.1 nm, comparable to that of the cholera toxin [9,10]. Due to the unknown and variable vertical compression, it is difficult to obtain a volume ratio among the subunits. But we do notice that the two large subunits are ~70% higher than the three small subunits.

On the original micrograph, the narrow gap between the subunits was found as small as 0.5 nm (Fig. 3a). But the same resolution was not clearly demonstrated on top of the subunits, perhaps because the contrast on the surface was too low, while between the subunits, the contrast was much higher, because the subunits could be pushed apart slightly. It is worth mentioning that the tip broadening is very small, in agreement with a previous finding [22]. In general, the height measured by AFM on soft materials is less accurate, due to the unknown amount of compression [21,26–31]. In this case, the best we obtained is about 2 nm on the pertussis toxin B-pentamers (Fig. 3b), which is nearly a 50% compression, based on the known structure of the cholera toxin [9,10]. It is worth noting that the lateral resolution is not seriously degraded, even under such a large vertical compression, which is consistent with a computer model (Yang and Shao, unpublished).

The B-pentamer was found quite stable in elevated temperatures up to 60°C. But, after 10 min treatment at 70°C, the majority of the subunits became dissociated (Fig. 4a). Due to the high coverage, whether S2 and S4, and S3 and S4 still remained in the dimer state cannot be determined. As a comparison, Fig. 4b is an image of the B-oligomer, after treatment at 60°C, where the structure remained intact. When the B-oligomer was treated by various pH solutions, the structure remained intact between pH 4.5–9.5 without appreciable dissociation of individual subunits. These results seem to indicate that at least the B-oligomer is rather stable under diverse environmental conditions. But we cannot rule out that the biological function of the pertussis toxin is already diminished at much milder conditions. Beyond this range, no stable image was obtained.

In conclusion, we have determined by in situ AFM that the B-oligomer of the pertussis toxin has a flat pentameric structure. Within the resolution limit of the AFM, the two large subunits, S2 and S3, appeared to be

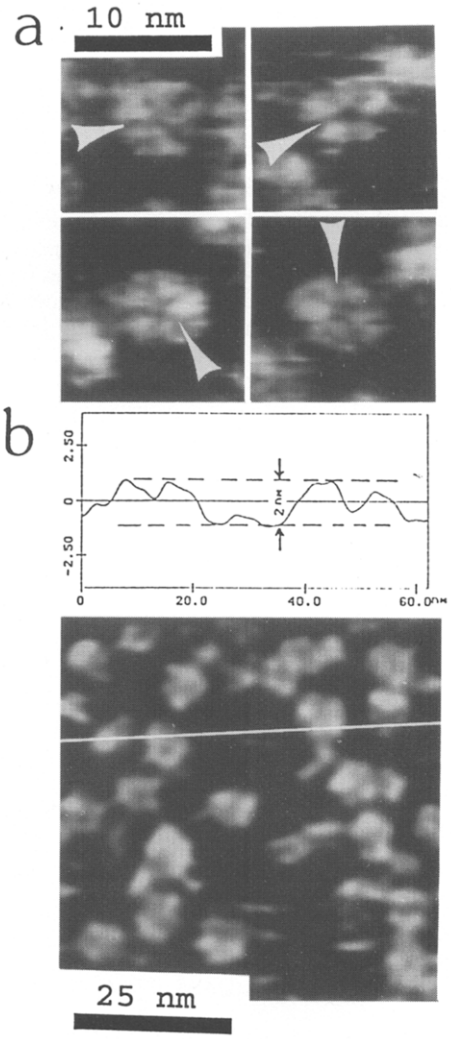

Fig. 3. (a) 4 images of the pertussis toxin B-oligomer zoomed up to show details (original data without any processing). The arrows indicate a gap of about 0.5 nm, demonstrating the remarkable resolving power of the AFM. (b) The top panel shows the height profile along the line drawn in the image below. The height measured on these pertussis toxin B-oligomers is about 2 nm, about 50% vertical compression, based on known cholera toxin structure.

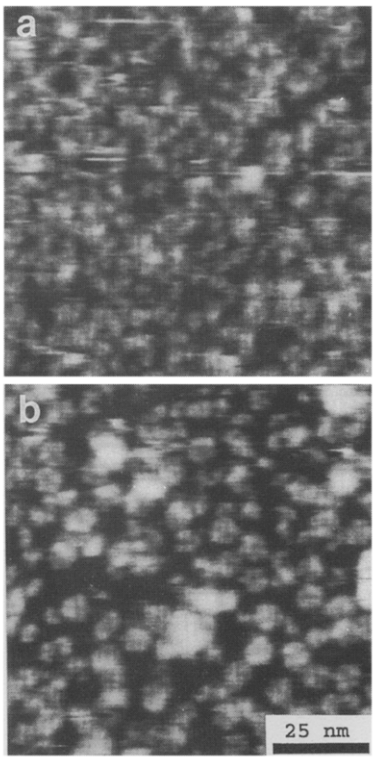

Fig. 4. (a) An image of the B-oligomer after treatment at 70°C. This image clearly shows that the subunits became dissociated at this temperature. Due to the high coverage, whether S2 and S4, as well as S3 and S4, was in the dimer state is not resolved. It is a surprise that even without any covalent bonding between the subunits, the B-pentamer could withstand such hash treatment. (b) An image of the pertussis toxin B-oligomer after treatment at 60°C. It is seen that the pentamer remained intact, but contrast is lower than that of Fig. 1a, which might be an indication of some damage to the molecules. This result does not rule out the possibility that the biological function is already diminished at much milder conditions.

next to each other. The catalytic A subunit is centrally located on top of the B-pentamer. The B-pentamer remains structurally intact for temperatures up to 60°C, and the pH between 4.5 and 9.5. We further demonstrated that the AFM is capable of a resolution down to the sub-nm range on these macromolecules directly adsorbed on mica surface, which opens the possibility of structural elucidation of other macromolecules, particularly for those that do not form two dimensional crystals or are sensitive to dehydration.

Acknowledgments: We thank Drs. D.L. Stokes, L.K. Tamm, A.P. Somlyo and A.V. Somlyo for useful discussions. We also thank S. Majewski and Ying Wu for technical assistance. Support from Whitaker Foundations, US Army Research Office (DAAL03-92-G-0002), National Science Foundation (BIR-9115655) and National Institutes of Health (RO1-RR07720 and PO1-HL48807) is gratefully acknowledged.

References

[1] Wardlaw, A.C. and Parton, R. (1988) Pathogenesis and Immunity in Pertussis, John Wiley & Sons Ltd., Chichester.
[2] Locht, C. and Keith, J. (1986) Science 232, 1258–1264.
[3] Tamura, M., Nogimori, K., Murai, S., Yajima, M., Ito, K., Katada, T. and Ui, M. (1982) Biochemistry 21, 5516–5522.
[4] Middlebrook, J.L. and Dorland, R.B. (1984) Microbiol. Rev. 48, 199–221.
[5] Moss, J. and Vaughan, M. (1988) Adv. Enzym. 61, 303–379.
[6] Spangler, B.D. (1992) Microbiol. Rev. 56, 622–647.
[7] Holmgren, J. (1981) Nature 292, 413–417.
[8] Sixma, T.K., Pronk, S.E., Kalk, K.H., Wartna, E.S., van Zanten, B.A.M., Witholt, B. and Hol, W.G.J. (1991) Nature 351, 371–377.
[9] Sixma, T.K., Stein, P.E., Hol, W.G.J. and Read, R.J. (1993) Biochemistry 32, 191–198.
[10] Ribi, H.O., Ludwig, D.S., Mercer, K.L., Schoolnik, G.K. and Kornberg, R.D. (1988) Science 239, 1272–1276.
[11] Tamura, M., Nogimori, S., Yajima, M., Ase, K. and Ui, M. (1983) J. Biol. Chem. 258, 6756–6761.
[12] Hausman, S.Z. and Burns, D.L. (1993) Infection and Immunity 61, 335–337.
[13] Morse, S.I. and Morse, J.H. (1976) J. Exp. Medicine 143, 1483–1502
[14] Binnig, G., Quate, C.F. and Gerber, Ch. (1986) Phys. Rev. Lett. 56, 930–933.
[15] Hansma, P.K., Elings, V.B., Marti O. and Bracker, C.E. (1988) Science 242, 209–214.
[16] Drake, B., Prater, C.B., Weisenhorn, A.L., Gould, S.A.C., Albrecht, T.R., Quate, C.F., Cannell, D.S., Hansma, H.G. and Hansma, P.K. (1989) Science 243, 1586–1589.
[17] Butt, H.-J., Downing, K.H. and Hansma, P.K. (1990) Biophys. J. 58, 1473–1480.
[18] Hoh, J.H., Lal, R., John, S.A., Revel, J.-P. and Arnsdorf, M F. (1991) Science 253, 1405–1408.
[19] Hoh, J.H. and Hansma, P.K. (1992) Trends Cell Biol. 2, 208–213.
[20] Yang, J., Tamm, L.K., Tillack, T.W. and Shao, Z. (1993) J. Mol. Biol. 229, 286–290.
[21] Yang, J., Tamm, L.K., Somlyo, A.P. and Shao, Z. (1993) J. Microscopy 171, 183–198.
[22] Hoh, J.H., Sosinsky, G.E., Revel, J.-P. and Hansma, P.K. (1993) Biophys. J. 65, 149–163.
[23] Yang, J., Mou, J. and Shao, Z. (1993) Biochem. Biophys. Acta, in press.
[24] Frank, J., Shimkin, B. and Dowse, H. (1981) Ultramicroscopy 6, 343–358.
[25] Frank, J. (1989) Electron Microsc. Rev. 2, 53–74.
[26] Lyubchenko, Y.L., Oden, P.I., Lampner, D., Lindsay, S.M. and Dunker, K.A. (1993) Nucleic Acids Res. 21, 1117–1123.
[27] Bustamante, C., Vesenka, J., Tang, C.L., Rees, W., Guthod, M. and Keller, R. (1992) Biochemistry 31, 22–26.
[28] Hansma, H.G., Vesenka, J., Siegerist, C., Kelderman, G., Morrett, H., Sinsheimer, P.L., Elings, V., Bustamante, C. and Hansma, P.K. (1992) Science 256, 1180–1184.
[29] Vesenka, J., Guthold, M., Tang, C.L., Keller, D., Delaine, E. and Bustamante, C. (1992) Ultramicroscopy 42–44, 1243–1249.
[30] Yang, J. and Shao, Z. (1993) Ultramicroscopy 50, 157–170.
[31] Rees, W.A., Keller, R.W., Vesenka, J., Yang, G. and Bustamante, C. (1993) Science 260, 1646–1649.